Collisional Transfer between Λ-Doublet Levels of OH($X^2\Pi_{3/2}$, $v = 1$, $j = 3.5$, and 6.5) in Collisions with He, Ar, N_2, and HNO_3†

Kevin M. Hickson, Chester M. Sadowski,‡ and Ian W. M. Smith*

School of Chemical Sciences, The University of Birmingham, Edgbaston, Birmingham B15 2TT, United Kingdom

Received: February 20, 2002; In Final Form: May 13, 2002

Using an infrared−ultraviolet double resonance method, we have measured rate coefficients at room temperature for the transfer of OH radicals between the Λ-doublet levels associated with the $j = 3.5$ and $j = 6.5$ rotational levels of the $X^2\Pi$, $\Omega = {}^3/_2$, $v = 1$ vibronic state in collisions with He, Ar, N_2, and HNO_3. OH radicals were generated by 266 nm pulsed laser photolysis of HNO_3 and promoted to selected Λ-doublet levels in $j = 3.5$ and $j = 6.5$ using a pulsed infrared laser tuned to the appropriate line in the (1, 0) infrared fundamental band of OH. The evolution of population in each Λ-doublet component of the selected rotational line was then observed using time-delayed laser-induced fluorescence in the (1, 1) band of the $A^2\Sigma^+ - X^2\Pi$ system. The measured rate coefficients (k_Λ) show a strong dependence on collision partner with $k_\Lambda(\text{He}) < k_\Lambda(\text{Ar}) < k_\Lambda(N_2) \ll k_\Lambda(HNO_3)$ and a significant dependence on rotational level, with the values of k_Λ larger for $j = 3.5$ than for $j = 6.5$, especially for HNO_3 as the collision partner.

I. Introduction

The dynamics of collisions between noble gas atoms and diatomic molecules in electronic states with both *S*, the total spin quantum number, and Λ, the projection of the orbital angular momentum, greater than zero have attracted considerable attention in recent years from both experimentalists and theoreticians. As with molecules in $^1\Sigma^+$ electronic states, collisions can bring about rotational energy transfer. In addition, however, in states with both S and $\Lambda > 0$, collisions can bring about changes in fine structure states (i.e., with different values of Ω) and the rotational levels are split by Λ-doubling. Experiments and calculations can examine the rate coefficients or cross-sections for collisional transfer between states that are defined with respect to these properties as well as the overall molecular rotation. Although classical theories can quite successfully model some aspects of these molecular collisions, for example, the transfer of molecules between rotational levels within the same fine structure or spin−orbit component of the given electronic state, quantum scattering calculations are required to tackle the more subtle aspects of collisional energy transfer.

Modern experiments on the collisional transfer of molecules between defined levels within the electronic ground state are of two kinds and provide complementary information.[1] In the first type of experiment, crossed supersonic beams are used, one of which is seeded with the species that is to be studied. This molecule is so strongly cooled in the supersonic expansion that significant populations remain only in the lowest two or three rotational levels. *Relative* values of integral and differential cross-sections can then be inferred by observing the molecules scattered into other levels by collisions with species in the second beam, using laser-induced fluorescence (LIF) or resonance-enhanced multiphoton ionization (REMPI) spectroscopy. The great strength of crossed molecular beam experiments is that one observes the result of single collisions that occur with a well-defined relative velocity and such experiments are capable of providing information of exquisitely fine detail about the results of inelastic collisions. For example, the use of electrical fields allows molecules to be aligned, oriented and further state-selected, and the use of polarized lasers for excitation or observation allows vector aspects of the scattering to be examined. However, molecular beam experiments do have some serious limitations. Most importantly, it is generally impossible to measure *absolute* values of the state-to-state cross-sections, a shortcoming that hampers comparison with theory. Second, initial state selection is severely constrained. Generally, population is drained into the lowest (or lowest few) rotational levels by the drastic cooling that occurs in the supersonic expansion. This means that information can only be obtained about collision-induced transitions out of this lowest level.

In experiments of the second kind, double resonance (DR) techniques are employed on thermally equilibrated samples. Either direct absorption of radiation from a tuneable infrared laser, Raman pumping, or stimulated emission pumping is used to promote a subset of molecules to a specific rovibrational level and a spectroscopic technique, such as LIF, is used to observe the re-distribution of these molecules as collisions occur. Such experiments yield *absolute* values of the rate coefficients: (i) for *total* transfer out a selected state, and (ii) for transfer between defined initial and final states. In comparison with experiments that use molecular beams to provide state-selection, such experiments have two distinct advantages. First, they provide *absolute* values of the rate coefficients for comparison with theory. Second, they can provide information about inelastic scattering from a wide range of initial rotational levels. On the other hand, no information is obtained about the dependence of transfer rates on the collision energy.

Experiments of one or other, or both types, have been used to investigate the details of rotational energy transfer in collisions of $NO(X^2\Pi_\Omega)$,[2−13] $OH(X^2\Pi_\Omega)$,[14−18] and $CN(A^2\Pi_\Omega)$.[19] Because

† Part of the special issue "Donald Setser Festschrift".

* To whom correspondence should be addressed. E-mail: i.w.m.smith@bham.ac.uk.

‡ On sabbatical leave from Department of Chemistry, York University, Toronto, Ontario, Canada M3J 1P3.

10.1021/jp0204859 CCC: $22.00
Published on Web 07/09/2002

of its stability, experiments on NO($X^2\Pi_\Omega$) are the most straightforward. Numerous measurements, using both the DR technique[1,2] and crossed molecular beams,[3−13] have been carried out. In many cases, the experimental results have been compared with state-of-the-art quantum scattering calculations on ab initio surfaces. Calculations by Alexander and co-workers show that when a diatomic species in a $^2\Pi$ state interacts with a noble gas atom, two potential energy surfaces (A' and A'') arise.[20] Furthermore, transfer between levels within the same spin−orbit manifold of rotational levels is determined by the *average* potential, i.e., $^1/_2$ ($A' + A''$), whereas transfer between levels within different spin−orbit manifolds is determined by the *difference* potential, i.e., $^1/_2$ ($A' - A''$).[21] Of special relevance to the present work, Alexander's calculations showed that transfer between specific rotational levels, in the same and different fine structure states, can show quite strong propensities in respect of the Λ-doublets, although, according to the calculations of Esposti et al.[22] on collisions between OH($X^2\Pi_\Omega$) and Ar and OH($X^2\Pi_\Omega$) and He, the *overall* rates of transfer from each j level differ only slightly for the e and f Λ-doublets.

In the present paper, we report the results of double resonance experiments that examine the transfer of OH radicals between Λ-doublets associated with the $j = 3.5$ ($N = 3$) and $j = 6.5$ ($N = 6$) levels in the ($X^2\Pi$, $\Omega = ^3/_2$, $v = 1$) vibronic state. As well as being of fundamental interest, the collisional properties of OH($X^2\Pi_\Omega$) are important in respect of observations of OH in highly excited rotational levels at high altitudes in the Earth's atmosphere[23] and, possibly, in respect of the OH astronomical maser.[24] In our experiments, OH radicals are created by pulsed laser photolysis of HNO_3. Some small fraction of these radicals are then promoted to a specific Λ-doublet level by absorption of radiation from a pulsed, tuneable, infrared laser, and the evolution of population, both in the Λ-doublet that is directly populated and in the other Λ-doublet of the same rovibronic level, is observed using LIF in appropriate lines of the (1,1) band in the $A^2\Sigma^+ - X^2\Pi$ electronic system of OH. We report rate coefficients for transfer between the Λ-doublet levels in collisions of OH with HNO_3, the photolytic source of OH radicals, He, Ar, and N_2.

II. Spectroscopy and Data Analysis

The nature, and particularly the symmetry, of the Λ-doublets associated with the rotational levels of molecules in $^2\Pi$ states have been discussed in a number of papers in the literature.[25−27] The levels of OH have attracted particular attention since unequal populations in the two Λ-doublets are a manifestation of two different orientations of a singly populated $p\pi$ orbital and can therefore contain important dynamical information when the OH radicals have been formed in a photochemical or chemical reaction. A summary, sufficient to understand the spectroscopy associated with levels involved in the studies reported here, is now given.

The two spin−orbit components of the $^2\Pi$ ground state of OH are "inverted", so that the F_1 levels with $N = j - ^1/_2$ belong to the lower $\Omega = ^3/_2$ component, and the F_2 levels with $N = j + ^1/_2$ belong to the upper $\Omega = ^1/_2$ component. Every rotational level is split into two closely spaced Λ-doublets, the two levels corresponding to different linear combinations of $+\Lambda$ and $-\Lambda$ projections of the electronic orbital angular momentum. The magnitude of the Λ-doublet splitting increases with increasing N, and is accompanied by a transition from Hund's case (a) to case (b). In the $^2\Pi_{3/2}$ levels that are of primary interest here, the e Λ-doublets lie lower than the f Λ-doublets; this notation referring to the total parity, exclusive of rotation. In OH($X^2\Pi_{3/2}$), the wave functions are symmetric with respect to reflection for the e Λ-doublets and anti-symmetric for the f Λ-doublets.

Because of previous confusion regarding the labeling of Λ-doublets, Alexander et al.[27] recommended that the Λ-doublet levels of linear molecules with nonzero orbital angular momentum should be labeled $\Pi(A')$ or $\Pi(A'')$ according to whether, for a given series of levels, the electronic wave function at high j is symmetric or anti-symmetric with respect to reflection of the spatial coordinates of the electrons in the plane of rotation. In this notation, in the F_1 levels of OH($X^2\Pi_{3/2}$), the e levels at high j have electronic wave functions which become symmetric with respect to reflection of the spatial coordinates of the electrons in the plane of rotation and they are labeled $\Pi(A')$. The f levels then correspond to those labeled $\Pi(A'')$. However, as emphasized by Andresen and Rothe,[26] at lower j the lobes of the $p\pi$ orbitals are less well oriented. Consequently, the observation of different Λ-doublet populations is not necessarily an indication of strong dynamic preferences.

Observing the kinetic behavior of the population in a particular Λ-doublet level is relatively straightforward. Electronic transitions to the $A^2\Sigma^+$ state from the F_1 levels of $X^2\Pi$, $v = 1$ level give rise to three main branches, P_{11}, Q_{11}, and R_{11}, in which changes in j and N are the same, together with an equal number of "satellite" branches $^qP_{21}$, $^rQ_{21}$, and $^sR_{21}$. However, the main Q-branch lines originate from the higher (f) Λ-doublets, whereas the main P-branch and R-branch lines originate from the lower (e) Λ-doublets. Consequently, it is straightforward to monitor the evolution of population in individual Λ-components; high spectral resolution is not required.

The situation is rather different in respect of the infrared transitions that are used to promote OH radicals to a specific Λ-doublet associated with a selected rotational level. Here we use lines in the (1,0) infrared fundamental band in OH; in effect, a $^2\Pi_{3/2}$-$^2\Pi_{3/2}$ transition. Now the spectrum consists of P-, Q-, and R-branches. Each branch contains lines from both Λ-doublets in the rotational levels of the lower ($v = 0$) vibrational level, so that each P-, Q-, and R-branch line is split into two, as a result of transitions from the different Λ-doublets in the ($v = 0, j''$) level. However, because of the $+ \leftrightarrow -$ selection rule, the splitting in the spectroscopic transitions is dependent on the particular branch to which a line belongs. Q-branch lines are more easily resolved because the allowed transitions join the lower (e) Λ-doublet in the ($v = 0, j''$) level to the upper (f) Λ-doublet in the ($v = 1, j'$) level and the upper (f) Λ-doublet in the ($v = 0, j''$) level to the lower (e) Λ-doublet in the ($v = 1, j'$) level. Consequently, the spectroscopic splitting corresponds to the *sum* of the level splittings in the upper (j') and lower (j'') levels. On the other hand, the P- and R-branch lines connect e to e and f to f, so that the spectroscopic splitting corresponds to the *difference* in the level splittings. This situation is represented in Figure 1 which also shows the splittings in the infrared lines used to promote OH radicals to specific Λ-doublets associated with the $j = 3.5$ ($N = 3$) and $j = 6.5$ ($N = 6$) in the ($X^2\Pi$, $\Omega = ^3/_2$, $v = 1$) vibronic level. For the lower rotational level, we used the Q-branch lines split by 0.866 cm^{-1}; for the higher rotational level, where the Λ-doublet splitting is greater in both the j' and the j'' levels, we used R-branch transitions that are split by 0.43 cm^{-1}.[28]

In most of our experiments, we fixed the frequency of the probe laser to a transition in the $A^2\Sigma^+ - X^2\Pi(1,1)$ band from a single Λ-doublet level of the ($X^2\Pi_{3/2}$, $v = 1$, j_i) level directly populated by the infrared pumping. We then performed two experiments in quick succession in which the intensity of the

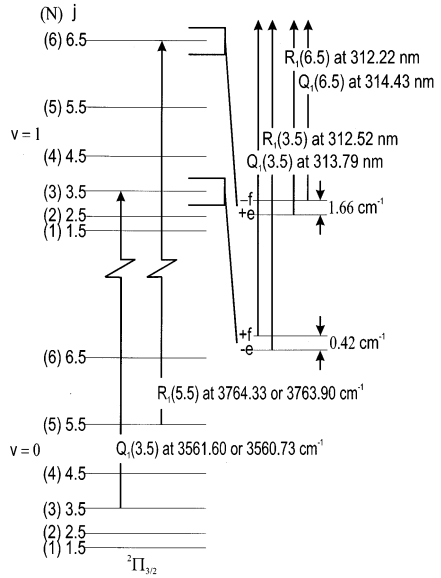

Figure 1. Energy level diagram for OH($X^2\Pi$) showing the levels in $\Omega = {}^3/_2$; $v = 0$ and 1. The manifold on the left gives no indication of Λ-doubling. The Λ-doublets in $X^2\Pi_{3/2}$, $v = 1$ between which collisional transfer is induced are shown and labeled on an expanded scale on the right. The transitions identified on the right are those used to probe level populations via transitions in the $A^2\Sigma^+ - X^2\Pi$ (1,1) band.

LIF signals was recorded as a function of delay between the pump and probe lasers with the infrared frequency tuned to correspond to excitation to one or other of the two Λ-doublet levels. In a smaller number of experiments, the frequency of the pump laser was kept constant and the frequency of the probe laser changed between the two experiments to record LIF traces reflecting population changes in the two Λ-doublet levels. An example of the two LIF traces obtained in the first kind of experiment is shown in Figure 2.

The objective of the present measurements was to obtain rate coefficients for the collisional transfer of OH between selected pairs of Λ-doublet levels within the same rotational level; i.e., the same j. To do this, we assumed a kinetic model based on the following scheme:

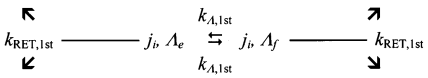

Here, j_i, Λ_e, and j_i, Λ_f represent populations in the e and f Λ-doublet levels of the rotational level j_i in ($X^2\Pi_{3/2}$, $v = 1$), $k_{\Lambda,1st}$ is the pseudo-first-order rate coefficient for transfer between these Λ-doublets, assumed to be equal in the two directions, as the energy splitting is $\ll k_B T$, and $k_{RET,1st}$ is the pseudo-first-order rate coefficient for transfer out of the two Λ-doublet levels into other rotational levels. There is some evidence that the values of $k_{RET,1st}$ may depend slightly on the Λ-doublet level[22] but this is ignored in our analysis, whose main purpose is to establish values of k_Λ, the second-order rate coefficient for transfer between Λ-doublet levels, for different collision partners and for different j_i.

The full algebraic solution of the rate equations based on this scheme is well-known (see Appendix). Given our assumptions about the rate coefficients, the time dependent populations (N_t) in the e and f levels should follow the equation

$$N_t = \frac{1}{2} N_0 \{\exp(-k_{RET,1st}\, t) \pm \exp(-[k_{RET,1st} + 2\, k_{\Lambda,1st}]t)\} \quad (1)$$

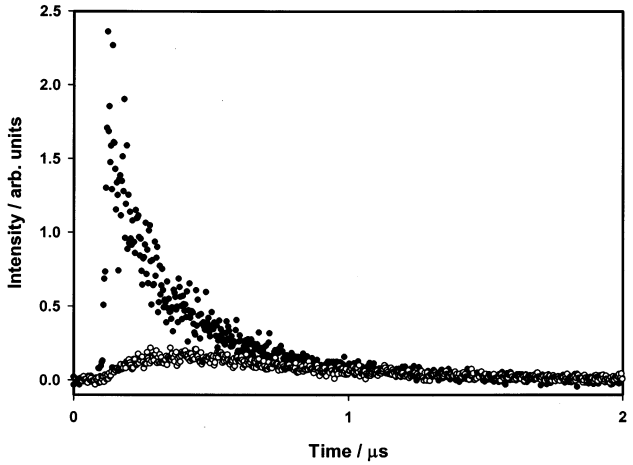

Figure 2. LIF signals reflecting changes in the populations of the f level of OH($X^2\Pi_{3/2}$, $v = 1$, $j = 6.5$). The closed circles show signals from the f level when it was directly populated by absorption of radiation from the IR pump laser; the open circles show signals from the f level when it was populated only by collision from the e level. The gas mixture contained 30 mTorr of HNO_3 in 570 mTorr of He.

Here, the + sign refers to the population in the Λ-doublet level that is directly populated by absorption of radiation from the pump level and the − sign refers to population in the other level. N_0 is the population initially produced in the Λ-doublet level that is directly populated. In practice, we have chosen to determine values of $k_{\Lambda,1st}$ by comparing the time evolution of the *ratio* (R) of the populations in the two Λ-doublet levels, thereby removing any explicit dependence of our results on $k_{RET,1st}$, the rate coefficient for rotational energy transfer. Taking R to be the ratio of the population in the Λ-doublet level that is only populated by collision to the population in the Λ-doublet level that is directly accessed by the pumping process, we can write, from eq 1

$$R = \frac{(1 - \exp(-2\, k_{\Lambda,1st} t))}{(1 + \exp(-2\, k_{\Lambda,1st} t))} \quad (2)$$

it is then easy to derive the equation

$$\ln\left(\frac{1-R}{1+R}\right) = -2\, k_{\Lambda,1st} t \quad (3)$$

These equations are used to analyze the results of the measurements on any given mixture. Derived values of $k_{\Lambda,1st}$ from experiments on different total pressures of the same mixtures of HNO_3 with diluent gas (M) are then plotted to obtain a second-order rate coefficient and the contribution of HNO_3 to transfer between Λ-doublets is then subtracted to yield the second-order rate coefficients for transfer between Λ-doublets in collisions between OH and M. Rate coefficients for transfer in collisions between OH and HNO_3 are determined from experiments on samples of pure HNO_3.

III. Experimental Method

The experiments were performed using the infrared−ultraviolet double resonance (IRUVDR) method in a manner similar to experiments on relaxation from high rotational levels of NO($X^2\Pi_{1/2}$) performed in this laboratory and reported by Islam et al.[2(f),2(g)]

Samples of pure HNO_3 or HNO_3 diluted (2−5%) in He, Ar, or N_2 were passed slowly through a cylindrical Pyrex cell fitted with a CaF_2 window, at the end where the photolysis and pump

lasers entered, and a Spectrosil B quartz window at the other end. The total pressure in the cell was monitored with a 10 Torr Baratron gauge. OH radicals were generated by partial photolysis of the HNO_3 using the radiation at 266 nm from a frequency-quadrupled Nd:YAG laser (Spectron Lasers, model SL803). Typical pulse energies of 20 mJ, a bandwidth of 0.4 cm^{-1}, and a fluence of ca. 30 J cm^{-2} were obtained. Using the absorption cross-section of HNO_3 at this wavelength ($\sigma_{266\ nm} = 1.76 \times 10^{-20}$ cm^2[29]), we estimate that ca. 0.05% of the HNO_3 was photolyzed in the cylindrical volume illuminated by the photolysis laser. This volume was only about a tenth of the total volume of the cell. Given a maximum residence time for the gas samples of 2 s, this means that the level of impurities was never more than ca. 0.1% of the concentration of HNO_3 and the effect of these impurities on the measurements could be safely neglected.

Pulses of tuneable infrared radiation were generated by difference-frequency mixing the output of a Nd:YAG pumped dye laser with the fundamental output of the same Nd:YAG laser Continuum ND8010/6000) in a $LiNbO_3$ crystal. The frequency of this IR pump laser was tuned into resonance with a line in the ($^2\Pi_{3/2}-^2\Pi_{3/2}$) sub-band of the (1,0) fundamental band of OH centered at 2.80 μm. The pulse energy was in the range from 3 to 4 mJ. The bandwidth was ca. 0.1 cm^{-1}, sufficient to resolve the individual components in the rotational lines that were used to promote OH radicals to a selected Λ-doublet. The wavenumbers of the pump transitions used in our experiments are given in Figure 1.

Tuneable UV probe radiation, with a bandwidth of ca. 0.4 cm^{-1}, was produced by frequency-doubling the output of a dye laser (Lambda-Physik, FL2002) pumped by an excimer laser operating at 308 nm on XeCl. This radiation was used to excite LIF in the (1,1) band of the $A^2\Sigma^+-X^2\Pi$ system of OH at ca. 314 nm. The wavelengths of the probe transitions used to observe the evolution of population in the *e* and *f* Λ-doublets of the $j = 3.5$ ($N = 3$) and $j = 6.5$ ($N = 6$) rotational levels in OH($X^2\Pi$, $\Omega = {}^3/_2$, $v = 1$) are given in Figure 1.

The beams from the photodissociation laser and the IR pump laser co-propagated along the axis of the cell, whereas the UV probe laser propagated in the opposite direction. The photomultiplier, an interference filter and a collecting lens were mounted in a housing which was clamped to the center of the cylindrical cell. Fluorescence was observed on resonance, i.e., in the (1,1) band, with a solar blind photomultiplier tube (Hamamatsu R801), through a quartz window and an interference filter (Corion, fwhm 10 nm) which discriminated against window fluorescence.

The equipment for controlling the firing of the lasers and for recording, accumulating and analyzing the LIF signals was the same as that described in previous papers from our laboratory.[2] The delay between the pulses from the photolysis and the IR probe lasers was set at 15 μs and the delays between the IR probe laser pulse and that from the UV probe were varied to a maximum of about 2 μs.

IV. Results

We have recorded LIF signals from specific Λ-doublets of the $j = 3.5$ and $j = 6.5$ rotational levels of OH($X^2\Pi_{3/2}$, $v = 1$) from samples of pure HNO_3 and from mixtures (≤5%) of HNO_3 in the diluent gases He, Ar and N_2. In most experiments, the wavelength of the probe laser was fixed to that of a particular R_1/P_1 transition (to observe population in the *e* Λ-doublet) or Q_1 (to observe population in the *f* Λ-doublet) in the (1,1) band of the $A^2\Sigma^+-X^2\Pi$ system of OH, as shown in Figure 1, and

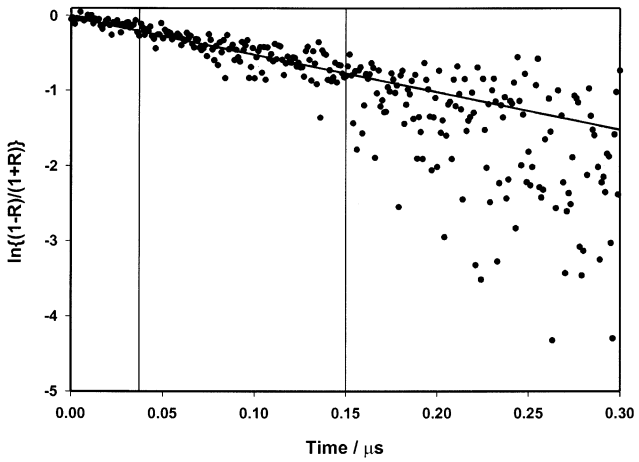

Figure 3. A plot showing the variation of the ratio of population (*R*) in the *e* Λ-doublet in OH($X^2\Pi_{3/2}$, $v = 1$, $j = 3.5$) with time following direct excitation of the *f* and the *e* Λ-doublets. In this representation, we show the variation of ln {(1 − R)/(1 + R)}with time and the straight line fit according to eq 3 for the points within the time interval defined by the two vertical lines. The raw data are from the same experiment on a mixture containing 6.8 mTorr HNO_3 at a total pressure of 370 mTorr, the diluent being N_2. The straight line fit yields the pseudo-first-order rate coefficient $k_{\Lambda,1st} = (5.1 \pm 0.5)$ μs^{-1}.

two LIF traces were recorded: one with the pump laser tuned to excite directly the Λ-doublet whose population was being observed and the other with the pump laser tuned to the other Λ-doublet so that the observed population was created only by collisions occurring in the gas sample. The required change in the wavenumber of the pump laser between the two IR transitions was, for both initial values of *j*, less than 1 cm^{-1} (see Figure 1), so the intensity of the pump laser, and hence the initially excited population (i.e., N_0 in eq 1) was the same in these two experiments. Care was taken to ensure that, in each of the measurements, the IR pump laser was tuned to the line center by maximizing the LIF signal.

In our analysis of the raw data, the initial 50−100 data points preceding the rising part of the signal pulse were used to calculate an average baseline, which was then subtracted from all the LIF intensities recorded in each of the two traces in each run. The zero of time was established at the onset of the rising part of the LIF signal from the Λ-doublet that was directly excited by the IR pump laser by inspection, and the ratio *R* of the Λ-doublet populations was then determined at all subsequent delay times. Only data points recorded well after the end of the pulse from the IR pump laser were used to determine the pseudo-first-order rate coefficients, $k_{\Lambda,1st}$. The values of *R* themselves were plotted versus time, when eq 2 was used to determine $k_{\Lambda,1st}$, and values of ln{(1 − *R*)/(1 + *R*)} were plotted versus time when eq 3 was used.

It is evident that errors in the ratio R increase with time as the populations in both the Λ-doublet levels decrease as a result of transfer to rotational levels other than j_i, Although eq 3 should result in a linear plot of ln{(1 − *R*)/(1 + *R*)} versus time, the fitting procedure is hampered by the drastic, and asymmetric, increase in uncertainty in ln{(1 − *R*)/(1 + *R*)} as *R* approaches unity at long delays. Consequently, these fits were constrained to relatively short delays for which $R \leq 0.4$ and ln{(1 − *R*)/(1 + *R*)} ≥ − 1. An example of such a fit, using only the points within the time interval defined by the vertical lines and applying a weighting to the points proportional to the reciprocal of the time delays at which they were recorded, is shown in Figure 3. This plot, and similar ones, confirm that the points are randomly scattered about the line of best fit within the portion of the trace

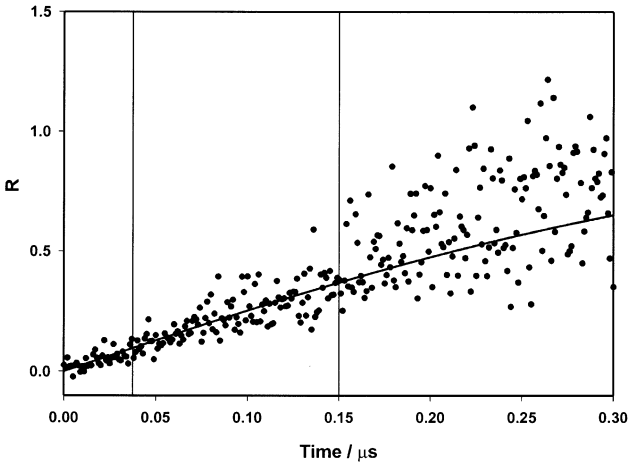

Figure 4. A plot showing the variation of the ratio of population (R) in the e Λ-doublet in OH($X^2\Pi_{3/2}$, $v = 1$, $j = 3.5$) with time following direct excitation of the f and the e Λ-doublets. In this representation, we show the variation of R with time with a fit of the form given in eq 2. Only the points within the time interval defined by the two vertical lines are fit The raw data are taken from the experiment on a mixture whose composition is given in the caption to Figure 3. The fit that is shown yields the pseudo-first-order rate coefficient $k_{\Lambda,1st} = (5.1 \pm 0.4)$ μs^{-1}.

defined above. At longer times, the individual errors increase rapidly with time and departures from linearity become evident.

These departures from linearity are to be expected due to the logarithmic nature of the function that is being plotted. They may also, in part, reflect limitations in the assumed kinetic model which does not allow for collisional re-population of the prepared j state. For these reasons, only the linear portions of the plots of $\ln\{(1 - R)/(1+ R)\}$ versus time, recorded at short delays, were used in the determination of pseudo-first-order rate constants. These portions of the plots were established by systematically deleting the data points at the tail of a plot until the fitted slope no longer decreased in a systematic way.

In Figure 4, we show the same set of data as that plotted in Figure 3 and extending over the same range of delay times fitted by use of eq 2. In this case, equal weights are attached to different values of R and a value of $k_{\Lambda,1st} = (5.1 \pm 0.4)$ μs^{-1} is obtained for the pseudo-first-order rate constant. This compares to a value of $k_{\Lambda,1st} = (5.1 \pm 0.5)$ μs^{-1} obtained from the use of eq 3. The exact agreement between this particular pair of values is undoubtedly fortuitous, but, in general, pairs of values obtained by these two fitting procedures agree well within their absolute uncertainties. As in Figure 3, the thin vertical lines in Figure 4 show the range of time delays over which data were fitted to yield values of $k_{\Lambda,1st}$.

In all, four different fitting procedures were compared with each other for a number of data sets. These procedures were comprised of fits based on eq 2 with constant fitting weights and with weight proportional to (1/time) and fits based on eq 3, again with constant fitting weights and with weights proportional to (1/time). All of these procedures yielded values of $k_{\Lambda,1st}$ for the experiments on pure HNO_3 that agreed with each other to within experimental error. Consequently, the decision was made to report the values for $k_{\Lambda,1st}$ obtained only by fitting eq 3 to the data with constant fitting weights.

To obtain second-order rate coefficients for the transfer between Λ-doublets in collisions with a specific collision partner, we plot the first-order rate coefficients obtained from several samples of the same gas at different total pressures against the total gas density. The individual values of $k_{\Lambda,1st}$ were given equal weight in these fits. In the case of samples of pure

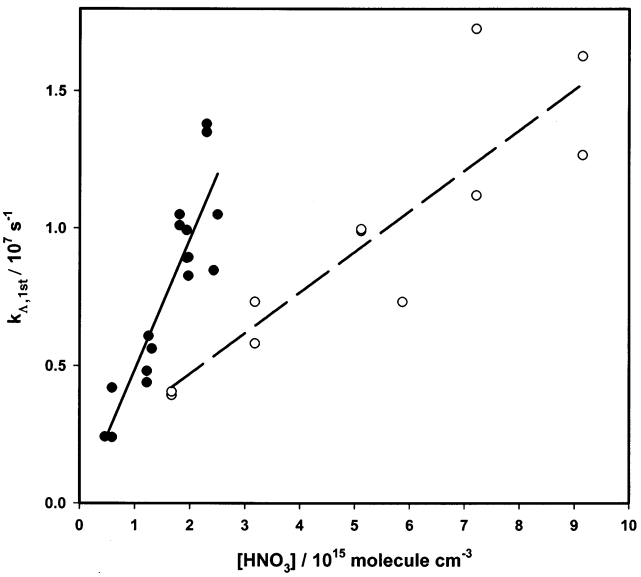

Figure 5. Plots of the pseudo-first-order rate coefficients, k_Λ, versus [HNO_3] for experiments on pure HNO_3. The filled circles and full line show results for OH($X^2\Pi_{3/2}$, $v = 1$, $j = 3.5$) and the open circles and dashed line show results for OH($X^2\Pi_{3/2}$, $v = 1$, $j = 6.5$). The gradients of the lines yield the second-order rate coefficients and errors given in Table 1.

HNO_3, such plots yield directly the second-order rate coefficients for transfer induced by collisions with HNO_3. Plots for $j = 3.5$ and $j = 6.5$ are shown in Figure 5. For mixtures of HNO_3 diluted in another gas (He, Ar, or N_2), a series of experiments were performed on the same gas mixture (i.e., containing the same mole fraction of HNO_3). The gradients of the lines plotted in Figure 6 correspond to an effective second-order rate constant (k_{eff}) for that particular mixture, where

$$k_{eff} = k_{\Lambda,HNO_3} X_{HNO_3} + k_{\Lambda,M} (1 - X_{HNO_3})$$

with X_{HNO3} equal to the mole fraction of HNO_3 in the gas mixture.

As the values of k_{Λ,HNO_3} are known from the experiments on pure HNO_3, it is then trivial to calculate the values of k_Λ for the diluent gases. Values of the rate coefficients for collisional transfer between the Λ-doublets of the $j = 3.5$ and $j = 6.5$ rotational levels of OH($X^2\Pi_{3/2}$, $v = 1$) are listed in Table 1. The errors that are quoted are single standard errors, the usual formulas being used to combine the errors from the measurements on gas mixtures and on pure HNO_3. The difficulty of obtaining actual values of the rate coefficients for He arises from the large difference between the efficiencies of HNO_3 and He in inducing transitions between Λ-doublets and, of course, the requirement to have enough HNO_3 present in the gas mixtures to generate observable concentrations of OH.

V. Discussion

There have been very few previous measurements of rate coefficients for Λ-doublet resolved collisional energy transfer in OH($X^2\Pi$), especially for transfer between the Λ-doublets associated with the same rotational level. The work closest to that described here is that reported about 10 years ago by Andresen and co-workers.[16(b)] Some of their experiments involved the selective creation of OH($X^2\Pi$) radicals in $\Omega = {}^3/_2$, $v = 0$, $j = 1.5$ in a supersonic expansion. The beam containing OH was intersected by a second beam, and excitation of the OH by collisions with H_2 or D_2 molecules in the second

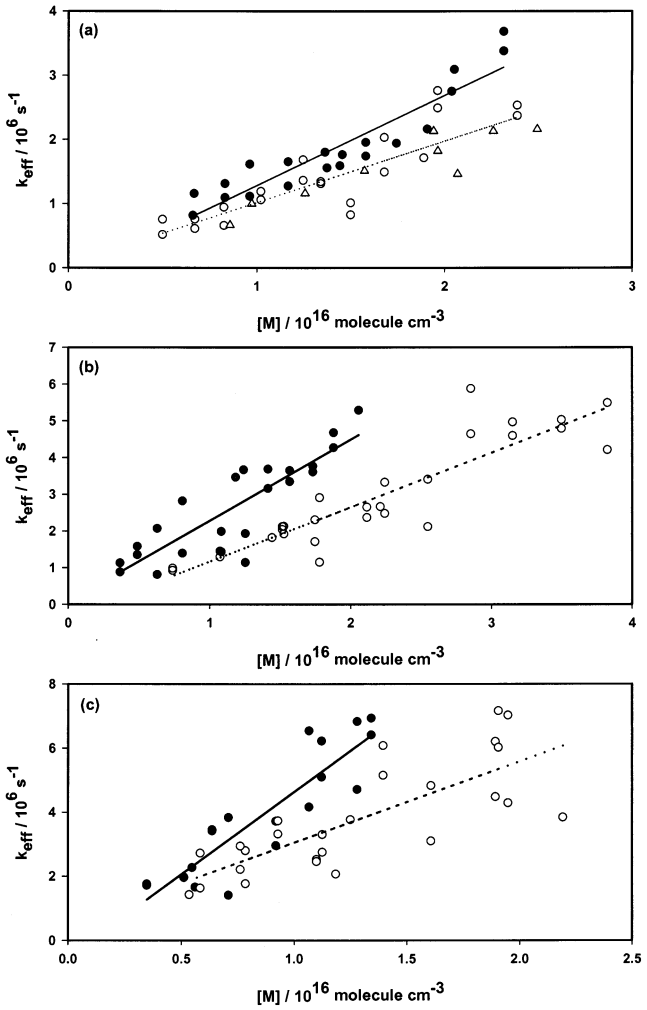

Figure 6. Plots of the pseudo-first-order rate coefficients, k_{eff}, versus total gas density [M] for mixtures containing 2−5% HNO_3 in the diluent gases: (a) He; (b) Ar; and (c) N_2. The filled circles and full lines show results for OH($X^2\Pi_{3/2}$, $v = 1$, $j = 3.5$) and the open circles and dashed lines show results for OH($X^2\Pi_{3/2}$, $v = 1$, $j = 6.5$). The triangles in (a) show the results of experiments in which the frequency of the IR laser was fixed to excite one Λ-doublet and the wavelength of the probe laser was chosen to monitor populations in each Λ-doublet in turn. After correction for the contributions of collisions with HNO_3 the gradients of the lines in these plots yield the second-order rate coefficients and errors given in Table 1.

TABLE 1: Rate Coefficients for the Transfer of OH Radicals between Λ-doublets Levels in the $j = 3.5$ and 6.5 Rotational Levels of the ($X^2\Pi_{3/2}$, $v = 1$) Vibronic State

	$k_\Lambda/10^{-10}$ cm^3 molecule^{-1} s^{-1}			
j	HNO_3	N_2	Ar	He
3.5	(24 ± 3)	(2.1 ± 0.3)	(0.5 ± 0.2)	
6.5	(7.5 ± 0.9)	(1.1 ± 0.3)	(0.3 ± 0.1)	(0.1 ± 0.1)

beam was probed by recording LIF spectra with and without the second beam "firing".

In a second series of experiments, closer in method and spirit to our own, they prepared OH in a flow system by pulsed laser photolysis of H_2O_2 and then performed IRUVDR experiments, similar to those described in the present paper. The rate coefficients that they extracted from their flow cell experiments were of limited accuracy. For transfer between the Λ-doublets associated with the $\Omega = {}^3/_2$, $v = 1$, $j = 1.5$ level in collisions with H_2, they found a value of $k_\Lambda = (5.1 \pm 1.1) \times 10^{-10}$ cm^3 molecule^{-1} s^{-1}. For the transfer between the Λ-doublets associated with $\Omega = {}^3/_2$, $v = 1$, $j = 4.5$, they found only rough values of k_Λ: $(0.1 - 5) \times 10^{-10}$ cm^3 molecule^{-1} s^{-1} for collisions with H_2 and $(1 - 10) \times 10^{-10}$ cm^3 molecule^{-1} s^{-1} for collisions with H_2O_2. In the context of our own results, we note (a) that H_2O_2, like HNO_3 apparently causes extremely rapid transfer between Λ-doublets in OH($X^2\Pi$), and (b) it appears that, for collisions with H_2, there is also a decrease in the rate coefficient, k_Λ, as the rotational level is increased.

At least three general features of our experimental results are worthy of note: (a) the sensitivity of the k_Λ values to collision partner, (b) the sensitivity of the k_Λ values to j, and (c) the magnitude of the rate coefficients with HNO_3 as collision partner (M). The rate coefficient with M = HNO_3 and $j = 3.5$ is equal to $(24 \pm 3) \times 10^{-10}$ cm^3 molecule^{-1} s^{-1}, and with M = HNO_3 and $j = 6.5$ it is $(7.5 \pm 0.9) \times 10^{-10}$ cm^3 molecule^{-1} s^{-1}. The rate coefficients correspond to thermally averaged cross-sections of approximately 350 Å^2 and 110 Å^2, respectively; values that are extraordinarily high for processes involving collisions between two electrically neutral species. It presumably reflects the fact that even a weak attractive force between these two strongly dipolar species is sufficient to promote transfer between the two, very nearly degenerate, Λ-doublet levels. We note again that the measurements of Andresen et al.[16(b)] indicate that H_2O_2 may be a similarly efficient collision partner for transfer between Λ-doublets.

The dependence of the k_Λ rate coefficients on rotational level, which is seen most dramatically in the data for M = HNO_3, cannot be explained on the basis of energetics; the splitting between the *e* and *f* levels in $v = 1$, $j = 6.5$ is only 1.66 cm^{-1}. The most likely explanation is the change in the nature of the Λ-doublet levels as j changes. For large values of the total angular momentum j, the Λ-doublet levels differ in respect of the orientation of the lobe of the $p\pi$ orbital containing the unpaired electron, either perpendicular to or in the plane of rotation and sometimes called[26] π^+ and π^-. However, this orientation is only well defined in the limit of high j. At lower j, the wave functions for the Λ-doublet levels are linear combinations of those for these orientations. Andresen et al.[26] have discussed this aspect of Λ-doubling in some detail. They define the *degree of electron alignment* as

$$\mathrm{DEA} = \frac{(\pi^+ - \pi^-)}{(\pi^+ + \pi^-)} \qquad (4)$$

For OH($X^2\Pi$), Andresen et al.[26] estimate that the degree of electron alignment varies from approximately 0.2 for $j = 1.5$ to 0.5 for $j = 3.5$ to 0.7 for $j = 6.5$. Our results suggest that transfer between Λ-doublet levels becomes less facile as the degree of electron alignment increases.

Our results for transfer between Λ-doublet levels in collisions with He and Ar can be compared with results from the elegant molecular beam experiments of ter Meulen and co-workers[17(c)] and with the calculations of Esposti et al.[22] Esposti et al. performed quantum scattering calculations on OH−He and OH−Ar collisions using potential energy surfaces (^{2}A′ and ^{2}A″) that were calculated using the coupled electron pair approximation (CEPA) and large basis set. Cross-sections for state-to-state transfer were calculated within the coupled states (CS) approximation, although the results of some of these calculations were tested by comparison with those from exact close-coupling (CC) calculations. For transfer between the *e* and *f* levels in OH($X^2\Pi_{3/2}$, $v = 2$, $j = 3.5$) in collisions with Ar, Esposti et al. reported a rate coefficient of 6.1×10^{-11} cm^3 molecule^{-1} s^{-1} at 300 K, which compares quite well with our experimental result of $(5 \pm 2) \times 10^{-11}$ cm^3 molecule^{-1} s^{-1} for OH($X^2\Pi_{3/2}$,

$v = 1$, $j = 3.5$). Results are not reported by Esposti et al. for Ar collisions with the OH radicals in initial levels above $j = 4.5$. However, the calculated rate coefficients for transfer between Λ-doublet levels in $X^2\Pi_{3/2}$, $v = 2$ decrease from 15.2 $\times$ 10^{-11} cm^3 molecule^{-1} s^{-1} for $j = 1.5$ to 4.0 $\times$ 10^{-11} cm^3 molecule^{-1} s^{-1} for $j = 4.5$, mirroring the decrease in k_Λ that we find between $X^2\Pi_{3/2}$, $v = 1$, $j = 3.5$ and $^2\Pi_{3/2}$, $v = 1$, $j = 6.5$ for all collision partners for which we can measure reliable data.

Esposti et al.[22] reported cross-sections, but not rate coefficients for collisions between OH and He. Like us, they found He to be appreciably less effective at transferring OH between Λ-doublet levels associated with the same value of j. Thus for OH($X^2\Pi_{3/2}$, $v = 0$, $j = 3.5$), they found a cross-section of 5.6 Å^2 at a collision energy of 300 cm^{-1}, compared with a value of 0.45 Å^2 for the same process at a collision energy of 394 cm^{-1} in collisions with He. The rate coefficients for these collision energies, i.e., the products of the cross-section and mean relative velocities, differ by a factor of about five, which is consistent with our finding for the thermally averaged rate coefficients.

The conclusion that He is much less effective than Ar in inducing transfer between Λ-doublet levels associated with the same j in OH($X^2\Pi_{3/2}$) is confirmed by the molecular beam experiments of ter Meulen and co-workers.[17(a)] Using supersonic expansion, followed by passage through a hexapole electric field, they were able to achieve 39.5% population in the upper (f,+) Λ-doublet level of OH($X^2\Pi_{3/2}$, $v = 0$, $j = 1.5$). The OH rotational state distribution was then probed, before and after collisions with He or Ar, by LIF spectroscopy. This allowed them to examine the same process as that studied in the present paper, namely the collisional transfer of OH molecules between Λ-doublets associated with the same value of j; in their case, $j = 1.5$ in $X^2\Pi_{3/2}$, $v = 0$. Unfortunately, their beautiful measurements suffered from the previously mentioned defect common to most crossed molecular beam experiments: the inability to derive absolute values of the cross-sections for transfer. To set their results on an absolute scale, they normalized them to the state-to-state cross-sections calculated by Esposti et al.[22] The agreement in the distribution of cross-sections for transfer to different final j and Λ-doublet states with both He and Ar as collision partners is excellent, supporting the accuracy of the calculations and the prediction that He is much less effective than Ar in inducing transfer between e and f components of the same j level.

Acknowledgment. We gratefully acknowledge a grant from The Leverhulme Trust in support of this work. We are also grateful to the EPSRC for successive loans from the Laser Loan Pool at the Rutherford-Appleton Laboratory.

Appendix

The evolution of the populations in two coupled states, each of which can be removed independently, has been treated many times, especially in regard to vibrational relaxation in the case where two molecules can exchange energy by a vibration-vibration exchange process as well as relaxing by vibration−translation relaxation of each excited species.[30] The present situation, without the approximations mentioned in the text, can be expressed by the scheme where additional subscripts

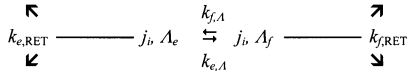

represent the Λ-doublet from which population is transferred or lost by the specified process, and all the rate coefficients in this scheme and elsewhere in this Appendix are pseudo-first-order rate coefficients. Solution of the kinetic equations in this case yields the following expressions for the populations in the two Λ-doublet levels

$$N = A\{\exp(-\lambda_1 t) \pm \exp(-\lambda_2 t)\} \tag{A1}$$

where the + sign refers to the population in the level populated at zero time by absorption of pulsed radiation and the − sign to the population in the other level. The values of A, λ_1, and λ_2 are given by the following equations

$$\lambda_2 = 0.5\{(k_{e\Lambda} + k_{f\Lambda} + k_{e,\mathrm{RET}} + k_{f,\mathrm{RET}}) + [(k_{e,\Lambda} + k_{e,\mathrm{RET}} - k_{f\Lambda} - k_{f,\mathrm{RET}})^2 + 4k_{e\Lambda}\,k_{f\Lambda}]^{1/2}\} \tag{A2}$$

and

$$\lambda_1 = 0.5\{(k_{e,\Lambda} + k_{f,\Lambda} + k_{e,\mathrm{RET}} + k_{f,\mathrm{RET}}) - [(k_{e,\Lambda} + k_{e,\mathrm{RET}} - k_{f,\Lambda} - k_{f,\mathrm{RET}})^2 + 4\,k_{e,\Lambda}k_{f,\Lambda}]^{1/2}\} \tag{A3}$$

The very small energy separation ($\Delta E \ll k_B T$) between the two Λ-doublets associated with the same rotational level in OH ($X^2\Pi$) and the principle of detailed balance fully justify the assumption that $k_{e,\Lambda} = k_{f,\Lambda} = k_\Lambda$ leading to a simplification of eqs A2 and A3

$$\lambda_2 = 0.5\{(2k_\Lambda + k_{e,\mathrm{RET}} + k_{f,\mathrm{RET}}) + [(k_{e,\mathrm{RET}} - k_{f,\mathrm{RET}})^2 + 4k_\Lambda{}^2]^{1/2}\} \tag{A4}$$

and

$$\lambda_1 = 0.5\{(2k_\Lambda + k_{e,\mathrm{RET}} + k_{f,\mathrm{RET}}) - [(k_{e,\mathrm{RET}} - k_{f,\mathrm{RET}})^2 + 4k_\Lambda{}^2]^{1/2}\} \tag{A5}$$

In terms of eq A1, R, the ratio of the population in the Λ-doublet level that is only populated by collision to the population in the Λ-doublet level that is directly accessed by the pumping process is given by

$$R = \frac{1 - \exp(-[\lambda_2 - \lambda_1]t)}{1 + \exp(-[\lambda_2 - \lambda_1]t)} \tag{A6}$$

When $k_{e,\mathrm{RET}} = k_{f,\mathrm{RET}}$, eq A6 reduces to

$$R = \frac{1 - \exp(-2k_\Lambda t)}{1 + \exp(-2k_\Lambda t)} \tag{A7}$$

which is eq 2 in the main text.

When $k_{e,\mathrm{RET}} \neq k_{f,\mathrm{RET}}$, $[\lambda_2 - \lambda_1]$ can be written as

$$[\lambda_2 - \lambda_1] = 2k_\Lambda\left(1 + \left[\frac{k_{e,\mathrm{RET}} - k_{f,\mathrm{RET}}}{2k_\Lambda}\right]^2\right)^{1/2} \tag{A8}$$

We note that, even with $(k_{e,\mathrm{RET}} - k_{f,\mathrm{RET}}) = 0.5\,k_\Lambda$, eq A8 would lead to $[\lambda_2 - \lambda_1] = 1.03 \times 2\,k_\Lambda$. The calculated values of Esposti et al.[22] for $J = 3.5$ and collisions of OH with Ar, yield ($k_{e,\mathrm{RET}} - k_{f,\mathrm{RET}}$) = 0.31 k_Λ, providing strong justification for the assumption in our analysis that $k_{e,\mathrm{RET}} = k_{f,\mathrm{RET}}$.

References and Notes

(1) Dagdigian, P. J. *The Chemical Dynamics and Kinetics of Small Radicals*; Liu, K., Wagner, A. F., Eds.; World Scientific: Singapore, 1995, Chapter 8; p 315.

(2) (a) Frost, M. J.; Islam, M.; Smith, I. W. M. *Can. J. Chem*. **1994**, *72*, 606; (b) Islam, M.; Smith, I. W. M.; Wiebrecht, J. W. *J. Phys. Chem*. **1994**, *98*, 9285; (c) Islam, M.; Smith, I. W. M.; Wiebrecht, J. W. *J. Chem. Phys*. **1995**, *103*, 9676; (d) James, P. L.; Sims, I. R.; Smith, I. W. M. *Chem. Phys. Lett.* **1997**, *272*, 412; (e) James, P. L.; Sims, I. R.; Smith, I. W. M.; Alexander, M. H.; Yang, M. *J. Chem. Phys.* **1998**, *109*, 3882; (f) Islam, M.; Smith, I. W. M.; Alexander, M. H. *Chem. Phys. Lett.* **1999**, *305*, 311; (g) Islam, M.; Smith, I. W. M.; Alexander, M. H. *Phys. Chem. Chem. Phys.* **2000**, *2*, 473.

(3) (a) Yang, X.; Wodtke, A. M. *J. Chem. Phys.* **1992**, *96*, 5123; (b) Yang, X.; Wodtke, A. M. *J. Phys. Chem*. **1993**, *97*, 3944.

(4) (a) Andresen, P.; Joswig, H.; Pauly, H.; Schinke, R. *J. Chem. Phys.* **1982**, *77*, 2204. (b) Joswig, H.; Andresen, P.; Schinke, R. *J. Chem. Phys.* **1986**, *85*, 1904.

(5) (a) Jons, S. D.; Shirley, J. E.; Vonk, M. T.; Giese, C. F.; Gentry, W. R. *J. Chem. Phys.* **1992**, *97*, 7831. (b) Jons, S. D.; Shirley, J. E.; Vonk, M. T.; Giese, C. F.; Gentry, W. R. *J. Chem. Phys.* **1996**, *105*, 5397.

(6) (a) Suits, A. G.; Bontoyan, L. S.; Houston, P. L.; Whitaker, B. J. *J. Chem. Phys.* **1992**, *96*, 8618. (b) Bontoyan, L. S.; Suits, A. G.; Houston, P. L.; Whitaker, B. J. *J. Phys. Chem.* **1993**, *97*, 6342.

(7) Meyer, H. *J. Chem. Phys.* **1995**, *102*, 3151.

(8) van Leuken, J. J.; van Ameron, F. H. W.; Bulthuis, J.; Snijders, J. G.; Stolte, S. *J. Phys. Chem.* **1995**, *99*, 15 573.

(9) Bieler, R.; Sanov, A.; Reisler, H. *Chem. Phys. Lett.* **1995**, *235*, 175.

(10) Lin, A.; Antonova, S.; Tsakotelli, A. P.; McBane, G. C. *J. Phys. Chem.* **1999**, *103*, 1198.

(11) Lorenz, K. T.; Chandler, D. W.; Barr, J. W.; Chen, W.; Barnes, G. L.; Cline, J. I. *Science* **2001**, *293*, 2063.

(12) Dixit, A. A.; Pisano, P. J.; Houston, P. L. *J. Phys. Chem.*, **2001**, *105*, 11 165.

(13) Barrass, P. A.; Sharkey, P.; Smith, I. W. M. *Phys, Chem. Chem. Phys.* **2002**, to be submitted.

(14) (a) Rensberger, K. J.; Jeffries, J. B.; Crosley, D. R. *J. Chem. Phys.* **1989**, *90*, 2174. (b) Raiche, G. A.; Jeffries, J. B.; Rensberger, K. J.; Crosley, D. R. *J. Chem. Phys.* **1990**, *92*, 7258. (c) Crosley, D. R.; Rensberger, K. J.; Jeffries, J. B. *Am. Inst. Phys. Conf. Proc.* **1989**, *191*, 615; (d) Wysong, I. J.; Jeffries, J. B.; Crosley, D. R. *J. Chem. Phys.* **1991**, *94*, 7547.

(15) Kliner, D. A. V.; Farrow, R. L. *J. Chem. Phys.* **1999**, *110*, 412.

(16) (a) Andresen, P.; Häusler, D.; Lülf, H. W. *J. Chem. Phys.* **1984**, *81*, 571. (b) Andresen, P.; Aristov, N.; Beushausen, V.; Häusler, D.; Lülf, H. W. *J. Chem. Phys.* **1991**, *95*, 5763.

(17) (a) Schreel, K.; Schleipen, J.; Eppink, A.; ter Meulen, J. J. *J. Chem. Phys.* **1993**, *99*, 8713. (b) Schreel, K.; ter Meulen, J. J. *J. Chem. Phys.* **1996**, *105*, 522. (c) Van Beek, M. C.; Schreel, K.; ter Meulen, J. J. *J. Chem. Phys.* **1998**, *109*, 1302. (d) Van Beek, M. C.; ter Meulen, J. J.; Alexander, M. H. *J. Chem. Phys.* **2000**, *113*, 628.

(18) Sonnenfroh, D. M.; Macdonald, R. G.; Liu, K. *J. Chem. Phys.* **1991**, *94*, 6508.

(19) (a) Yang, X.; Dagdigian, P. J. *Chem. Phys. Lett.* **1998**, *297*, 506. (b) Yang, X.; Dagdigian, P. J. *Chem. Phys. Lett.* **1999**, *305*, 311. (c) Yang, X.; Dagdigian, P. J.; Alexander, M. H. *J. Chem. Phys.* **2000**, *112*, 4474.

(20) Alexander, M. H. *Chem. Phys.* **1985**, *92*, 337.

(21) Alexander, M. H. *J. Chem. Phys.* **1982**, *76*, 5974.

(22) Esposti, A. D.; Berning, A.; Werner, H.-J. *J. Chem. Phys.* **1995**, *103*, 2067.

(23) Holtzclaw, K. W.; Upschulte, B. L.; Caledonia, G. E.; Croni, J. F.; Green, B. D.; Lipson, S. J.; Blumberg, W. A. M.; Dodd, J. A. *J. Geophys. Res*. **1997**, *102A*, 4521.

(24) (a) Reid, M. J.; Moran, J. M. *Annu. Rev. Astron. Astrophys.* **1981**, *19*, 231. (b) Elitzur, M. *Rev. Mod. Phys.* **1982**, *54*, 1225. (c) ter Meulen, J. J. in *Molecules in Astrophysics: Probes and Processes, IAU Sympos. 178*; van Dishoeck, E. F., Ed.; Kluwer: Dordrecht, 1997; p 241.

(25) Alexander, M. H.; Dagdigian, P. J. *J. Chem. Phys.* **1984**, *80*, 4325.

(26) Andresen, P.; Rothe E. W. *J. Chem. Phys*. **1985**, *82*, 3634.

(27) Alexander, M. H.; Andresen, P.; Bacis, R.; Bersohn, R.; Comes, F. J.; Dagdigian, P. J.; Dixon, R. N.; Field, R. W.; Flynn, G. W.; Gericke, K.-H.; Grant, E. R.; Howard, B. J.; Huber, R. J.; King, D. S.; Kinsey, J. L.; Kleinermanns, K.; Kuchitsu, K.; Lunz, A. C.; McCaffery, A. J.; Pouilly, B.; Reisler, H.; Rosenwaks, S.; Rothe, E. W.; Shapiro, M.; Simons, J. P.; Yasudev, R.; Wiesenfeld, J. R.; Wittig, C.; Zare, R. N. *J. Chem. Phys.* **1988**, *89*, 1749.

(28) Mélen, F.; Sauval, A. J.; Grevesse, N.; Farmer, C. B.; Servass, Ch.; Delbouille, L.; Roland, G. *J. Mol. Spectrosc.* **1995**, *174*, 490.

(29) Atkinson, R.; Baulch, D. L.; Cox, R. A.; Hampson, R. F., Jr.; Kerr, J. A.; Rossi, M. J.; Troe, J. *J. Phys. Chem. Ref. Data* **1997**, *26*, 521.

(30) Stephenson, J. C.; Moore, C. B. *J. Chem. Phys.* **1972**, *56*, 1295.